the operation and for 2 hours after MCA occlusion. The ratio of CBF after cell transplantation to CBF before cell transplantation was calculated to evaluate the change of CBF (termed relative CBF).

Analysis of perfusion and brain infarction after MCA occlusion. Carbon black ink (Fuekinori Kogyo Co. Ltd., Osaka, Japan) was used to delineate the perfused area after MCA ligation as described (42). Viability of brain tissue was evaluated using TTC (Sigma-Aldrich, St. Louis, Missouri, USA). Coronal sections (1 mm thick) of the forebrain were stained with 1% TTC, and the images of sections from the exact center of the forebrain were captured using a microscopic digital camera system (Olympus, Tokyo, Japan). The width of viable cortex was determined by NIH image.

Administration of CD34⁺ cells after stroke. CD34⁺ cells (containing Flk-1⁻ and Flk-1⁺ cell populations) and CD34⁺/Flk-1⁻ cells were isolated from cord blood using a Direct CD34 Progenitor Cell Isolation kit (Miltenyi Biotec, Bergisch Gladbach, Germany), CD34 Multisort kit (Miltenyi Biotec), and anti-Flk-1 antibody (Sigma-Aldrich), according to the manufacturers' protocols. CD34⁻ mononuclear cells were also collected for control experiments. In each case, cell populations were analyzed by FACS (BD Biosciences, San Jose, California, USA) using PerCP-conjugated anti-CD34 antibody (BD Biosciences), phycoerythrin-conjugated (PE-conjugated) anti-P1H12 antibody (BD Biosciences), and anti-Flk-1 antibody (Sigma-Aldrich) conjugated with FITC according to the manufacturer's protocol (Zenon Alexa Fluor; Molecular Probes Inc., Eugene, Oregon, USA). For labeling studies, cells were incubated with the fluorescent dye chloromethylbenzamido (CM-DiI; Molecular Probes Inc.). Forty-eight hours after stroke, 5×10^5 CD34⁺, CD34⁺/FLK-1⁻, CD34⁻ cells, or the same volume (100 μl) of PBS were infused intravenously via the tail vein.

For the analysis of the effect of aging on neurogenesis, 24-week-old male SCID mice were used. Because of the known increased evidence of tumors, infection (for example, excess mucus in the eye), and elevated plasma immunoglobulins in older SCID mice, the presence of each of these conditions was also investigated. Mice with evidence of weight loss, tumors, infection, or elevated plasma immunoglobulins (>10 μg/ml) were excluded from further analysis.

Immunohistochemistry. Mice brains were removed and fixed in paraformaldehyde. Coronal sections (20 μm) were prepared using a vibratome (Leica Microsystems Inc., Wetzlar, Germany). To assess cell proliferation and angiogenesis, fresh frozen sections (20 μm) were prepared and fixed in acetone. Sections were subjected to immunohistochemistry with antibody to NeuN (Chemicon International, Temecula, California, USA), mouse-specific antibody to CD31 (BD Biosciences), human-specific antibody to CD31 (DAKO A/S, Glostrup, Denmark), mouse-specific antibody to CD13 (Santa Cruz Biotechnology, Santa Cruz, California, USA), and antibodies to MAP-2 (Sigma-Aldrich), human von Willebrand Factor (DAKO A/S), PSA-NCAM (Chemicon International), DCX (Chemicon International), Musashi-1 (19), TUNEL (Molecular Probes Inc.), or BrdU (Boehringer Ingelheim, Ingelheim, Germany).

Cell proliferation analysis. For assessment of cell proliferation in vivo, BrdU (Sigma-Aldrich) was administered intraperitoneally. In the case of endothelial cell proliferation, BrdU (200 mg/kg) was administered 24 hours before killing. For endogenous neurogenesis, 50 mg/kg of BrdU was injected every second day for a total of 14 days. Cells co-staining for BrdU and mouse-specific antibody to CD31 using confocal microscopy (Olympus) in HPFs (×40 of objective lens) were counted as proliferating endothelial cells. The cell population co-staining for BrdU and NeuN was counted as regenerating-proliferating neurons. For quantitative analysis, brain sections at the exact center of the forebrain were stained, and the left cortical area of 1 mm (or >1 mm) distal from the midline was examined by two investigators blinded to the experimental protocol. In each case, 10 representative fields were evaluated before quantitative results were analyzed.

Assessment of angiogenesis. For assessment of angiogenesis at the border of MCA and ACA areas, carbon black perfusion was used to visualize the vasculature and TTC staining to demarcate the border of viable and non-viable tissue. Semi-quantitative analysis of angiogenesis made use of the angiographic score and was calculated by a previously described method (43). Microscopic digital images were scanned into a computer (Olympus), and an overlay, composed of 50-μm-diameter circles arranged in rows spaced 100 μm apart, was superimposed on the image. The total number of grids intersecting the border zone containing a microvessel was counted. Mouse-specific antibody to CD13 was used to visualize 'activated' vasculature.

Assessment of ischemic brain damage and neurogenesis. For determination of the cortical width index, whole-brain images were captured using a microscopic digital camera system (Olympus). The width at the midpoint of the forebrain was measured, and the ratio of left width to right width was defined as the cortical width index. To quantify accelerated neurogenesis, three brain sections around the center of the forebrain on day 14 after cell transplantation were stained with NeuN or TUNEL. The number of small NeuN nuclei-positive cells in the white matter at lower left of the left cortex and the number of TUNEL⁺ cells around the lower part of ischemic cortical edge was counted in HPFs. For determining the number of neurons in the left cortex, brain sections of the exact center of the forebrain on day 90 were stained with NeuN, and the total number of NeuN⁺ cells was quantitated.

Behavioral analysis. To assess cortical function, mice were subjected to behavioral testing in the open-field task (44) on day 35 or 90 after cell transplantation. Auditory startling behavior was tested as described (45). To estimate learning activity, mice were tested by water maze test (46) and passive avoidance test (47). To exclude the contribution of physical deficits directly related to the operative procedure and induction of stroke, motor deficiencies were examined on days 9 and 16 after stroke. Neurological deficits were scored on a three-point modified scale as described (17). Body weight, monitored in each experimental group, displayed no significant differences (data not shown).

Inhibition and promotion of neovascularization. Inhibition of neovascularization was achieved by administering Endostatin (10 μg; subcutaneous; Calbiochem-Novabiochem, Darmstadt, Germany) once daily for 14 days. To stimulate mobilization of EPCs originating in the host, EPO (1,000 μg/kg) was injected subcutaneously 24, 48, and 72 hours after ischemia. Peripheral blood cells were analyzed using FITC-conjugated anti-mouse CD45 (BD Biosciences), PE-conjugated anti-mouse CD34 antibodies (BD Biosciences), and 7-amino-actinomycin D viability Dye (Beckman Coulter Inc., Marseille Cedex, France), as described (48), using counting beads (BD Biosciences) as an internal control.

Data analysis. In all experiments, mean ± SE is reported. Statistical comparisons among groups were determined using one-way ANOVA. Where indicated, individual comparisons were performed using Student's *t* test.

Acknowledgments

Musashi-1 was generously provided by H. Okano at Keiou University in Japan. This work was partially supported by the Uehara, Takeda, and Terumo Medical Foundations, Grant-in-Aid for Scientific Research from the ministry of Education (15590785) and from the Ministry of Health, Labour, and Welfare (16C-7, H16-CK-004). We would like to thank Y. Kasahara, K. Obata, and Y. Okinaka for technical assistance.

Received for publication November 24, 2003, and accepted in revised form May 18, 2004.

Address correspondence to: Akihiko Taguchi, Department of Cerebrovascular Disease, National Cardiovascular Center, 5-7-1 Fujishiro-dai, Suita, Osaka 565-8565, Japan. Phone: 81-6-6833-5012; Fax: 81-6-6872-7485; E-mail: ataguchi@res.ncvc.go.jp.

1. Asahara, T., et al. 1997. Isolation of putative progenitor endothelial cells for angiogenesis. *Science.* 275:964–967.
2. Asahara, T., et al. 1999. Bone marrow origin of endothelial progenitor cells responsible for postnatal vasculogenesis in physiological and pathological neovascularization. *Circ. Res.* 85:221–228.
3. Kawamoto, A., et al. 2001. Therapeutic potential of ex vivo expanded endothelial progenitor cells for myocardial ischemia. *Circulation.* 103:634–637.
4. Majka, M., et al. 2001. Numerous growth factors, cytokines, and chemokines are secreted by human CD34$^+$ cells, myeloblasts, erythroblasts, and megakaryoblasts and regulate normal hematopoiesis in an autocrine/paracrine manner. *Blood.* 97:3075–3085.
5. Taguchi, A., Ohtani, M., Soma, T., Watanabe, M., and Kinosita, N. 2003. Therapeutic angiogenesis by autologous bone-marrow transplantation in a general hospital setting. *Eur. J. Vasc. Endovasc. Surg.* 25:276–278.
6. Tateishi-Yuyama, E., et al. 2002. Therapeutic angiogenesis for patients with limb ischaemia by autologous transplantation of bone-marrow cells: a pilot study and a randomised controlled trial. *Lancet.* 360:427–435.
7. Hamano, K., et al. 2001. Local implantation of autologous bone marrow cells for therapeutic angiogenesis in patients with ischemic heart disease: clinical trial and preliminary results. *Jpn. Circ. J.* 65:845–847.
8. Chen, J., et al. 2001. Intravenous administration of human umbilical cord blood reduces behavioral deficits after stroke in rats. *Stroke.* 32:2682–2688.
9. Hess, D.C., et al. 2002. Bone marrow as a source of endothelial cells and NeuN-expressing cells after stroke. *Stroke.* 33:1362–1368.
10. Nakatomi, H., et al. 2002. Regeneration of hippocampal pyramidal neurons after ischemic brain injury by recruitment of endogenous neural progenitors. *Cell.* 110:429–441.
11. Drago, J., Murphy, M., Carroll, S.M., Harvey, R.P., and Bartlett, P.F. 1991. Fibroblast growth factor-mediated proliferation of central nervous system precursors depends on endogenous production of insulin-like growth factor I. *Proc. Natl. Acad. Sci. U. S. A.* 88:2199–2203.
12. Jin, K., et al. 2002. Vascular endothelial growth factor (VEGF) stimulates neurogenesis in vitro and in vivo. *Proc. Natl. Acad. Sci. U. S. A.* 99:11946–11950.
13. Solovey, A., et al. 1997. Circulating activated endothelial cells in sickle cell anemia. *N. Engl. J. Med.* 337:1584–1590.
14. Bhagwat, S.V., Petrovic, N., Okamoto, Y., and Shapiro, L.H. 2003. The angiogenic regulator CD13/APN is a transcriptional target of Ras signaling pathways in endothelial morphogenesis. *Blood.* 101:1818–1826.
15. Van Dam, D., et al. 2003. Age-dependent cognitive decline in the APP23 model precedes amyloid deposition. *Eur. J. Neurosci.* 17:388–396.
16. Farkas, T., et al. 2003. Peripheral nerve injury influences the disinhibition induced by focal ischaemia in the rat motor cortex. *Neurosci. Lett.* 342:49–52.
17. Tamatani, M., et al. 2001. ORP150 protects against hypoxia/ischemia-induced neuronal death. *Nat. Med.* 7:317–323.
18. Iwai, M., et al. 2003. Temporal profile of stem cell division, migration, and differentiation from subventricular zone to olfactory bulb after transient forebrain ischemia in gerbils. *J. Cereb. Blood Flow Metab.* 23:331–341.
19. Sakakibara, S., et al. 1996. Mouse-Musashi-1, a neural RNA-binding protein highly enriched in the mammalian CNS stem cell. *Dev. Biol.* 176:230–242.
20. Arvidsson, A., Collin, T., Kirik, D., Kokaia, Z., and Lindvall, O. 2002. Neuronal replacement from endogenous precursors in the adult brain after stroke. *Nat. Med.* 8:963–970.
21. O'Reilly, M.S., et al. 1997. Endostatin: an endogenous inhibitor of angiogenesis and tumor growth. *Cell.* 88:277–285.
22. Capillo, M., et al. 2003. Continuous infusion of endostatin inhibits differentiation, mobilization, and clonogenic potential of endothelial cell progenitors. *Clin. Cancer Res.* 9:377–382.
23. Bahlmann, F.H., et al. 2004. Erythropoietin regulates endothelial progenitor cells. *Blood.* 103:921–926.
24. Jaquet, K., Krause, K., Tawakol-Khodai, M., Geidel, S., and Kuck, K.H. 2002. Erythropoietin and VEGF exhibit equal angiogenic potential. *Microvasc. Res.* 64:326–333.
25. Gage, F.H. 2000. Mammalian neural stem cells. *Science.* 287:1433–1438.
26. Yagita, Y., et al. 2001. Neurogenesis by progenitor cells in the ischemic adult rat hippocampus. *Stroke.* 8:1890–1896.
27. Ross, M.A., Sander, C.M., Kleeb, T.B., Watkins, S.C., and Stolz, D.B. 2001. Spatiotemporal expression of angiogenesis growth factor receptors during the revascularization of regenerating rat liver. *Hepatology.* 34:1135–1148.
28. Toda, S., et al. 1999. Immunohistochemical expression of growth factors in subacute thyroiditis and their effects on thyroid folliculogenesis and angiogenesis in collagen gel matrix culture. *J. Pathol.* 188:415–422.
29. Johe, K.K., Hazel, T.G., Muller, T., Dugich-Djordjevic, M.M., and McKay, R.D. 1996. Single factors direct the differentiation of stem cells from the fetal and adult central nervous system. *Genes Dev.* 10:3129–3140.
30. Leventhal, C., Rafii, S., Rafii, D., Shahar, A., and Goldman, S.A. 1999. Endothelial trophic support of neuronal production and recruitment from the adult mammalian subependyma. *Mol. Cell. Neurosci.* 13:450–464.
31. Araujo, D.M., and Cotman, C.W. 1993. Trophic effects of interleukin-4, -7 and -8 on hippocampal neuronal cultures: potential involvement of glial-derived factors. *Brain Res.* 600:49–55.
32. Valable, S., et al. 2003. Angiopoietin-1-induced PI3-kinase activation prevents neuronal apoptosis. *FASEB J.* 17:443–445.
33. Sun, W., Funakoshi, H., and Nakamura, T. 2002. Localization and functional role of hepatocyte growth factor (HGF) and its receptor c-met in the rat developing cerebral cortex. *Brain Res. Mol. Brain Res.* 103:36–48.
34. Louissaint, A., Jr., Rao, S., Leventhal, C., and Goldman, S.A. 2002. Coordinated interaction of neurogenesis and angiogenesis in the adult songbird brain. *Neuron.* 34:945–960.
35. Lo, E.H., Dalkara, T., and Moskowitz, M.A. 2003. Mechanisms, challenges and opportunities in stroke. *Nat. Rev. Neurosci.* 4:399–415.
36. Beck, H., et al. 2003. Participation of bone marrow-derived cells in long-term repair processes after experimental stroke. *J. Cereb. Blood Flow Metab.* 23:709–717.
37. Zhang, Z.G., Zhang, L., Jiang, Q., and Chopp, M. 2002. Bone marrow-derived endothelial progenitor cells participate in cerebral neovascularization after focal cerebral ischemia in the adult mouse. *Circ. Res.* 90:284–288.
38. Kondziolka, D., et al. 2000. Transplantation of cultured human neuronal cells for patients with stroke. *Neurology.* 55:565–569.
39. Hoehn, M., et al. 2002. Monitoring of implanted stem cell migration in vivo: a highly resolved in vivo magnetic resonance imaging investigation of experimental stroke in rat. *Proc. Natl. Acad. Sci. U. S. A.* 99:16267–16272.
40. Abe, K. 2000. Therapeutic potential of neurotrophic factors and neural stem cells against ischemic brain injury. *J. Cereb. Blood Flow Metab.* 20:1393–1408.
41. Matsushita, K., et al. 1998. Marked, sustained expression of a novel 150-kDa oxygen-regulated stress protein, in severely ischemic mouse neurons. *Brain Res. Mol. Brain Res.* 60:98–106.
42. Matsuyama, T., et al. 1983. Why are infant gerbils more resistant than adults to cerebral infarction after carotid ligation? *J. Cereb. Blood Flow Metab.* 3:381–385.
43. Takeshita, S., et al. 1994. Therapeutic angiogenesis. A single intraarterial bolus of vascular endothelial growth factor augments revascularization in a rabbit ischemic hind limb model. *J. Clin. Invest.* 93:662–670.
44. Kimble, D.P. 1968. Hippocampus and internal inhibition. *Psychol. Bull.* 70:285–295.
45. Sasaki, H., Iso, H., Coffey, P., Inoue, T., and Fukuda, Y. 1998. Prepulse facilitation of auditory startle response in hamsters. *Neurosci. Lett.* 248:117–120.
46. Balschun, D., et al. 2003. Does cAMP response element-binding protein have a pivotal role in hippocampal synaptic plasticity and hippocampus-dependent memory? *J. Neurosci.* 23:6304–6314.
47. Mereu, G., et al. 2003. Prenatal exposure to a cannabinoid agonist produces memory deficits linked to dysfunction in hippocampal long-term potentiation and glutamate release. *Proc. Natl. Acad. Sci. U. S. A.* 100:4915–4920.
48. Gratama, J.W., et al. 1999. Comparison of single- and dual-platform assay formats for CD34$^+$ haematopoietic progenitor cell enumeration. *Clin. Lab. Haematol.* 21:337–346.

Circulating CD34-Positive Cells Provide an Index of Cerebrovascular Function

Akihiko Taguchi, MD; Tomohiro Matsuyama, MD; Hiroshi Moriwaki, MD; Takuya Hayashi, MD; Kohei Hayashida, MD; Kazuyuki Nagatsuka, MD; Kenichi Todo, MD; Katsushi Mori; David M. Stern, MD; Toshihiro Soma, MD; Hiroaki Naritomi, MD

Background—Increasing evidence points to a role for circulating endothelial progenitor cells, including populations of CD34- and CD133-positive cells present in peripheral blood, in maintenance of the vasculature and neovascularization. Immature populations, including CD34-positive cells, have been shown to contribute to vascular homeostasis, not only as a pool of endothelial progenitor cells but also as a source of growth/angiogenesis factors at ischemic loci. We hypothesized that diminished numbers of circulating immature cells might impair such physiological and reparative processes, potentially contributing to cerebrovascular dysfunction.

Methods and Results—The level of circulating immature cells, CD34-, CD133-, CD117-, and CD135-positive cells, in patients with a history of atherothrombotic cerebral ischemic events was analyzed to assess possible correlations with the degree of carotid atherosclerosis and number of cerebral infarctions. There was a strong inverse correlation between numbers of circulating CD34- and CD133-positive cells and cerebral infarction. In contrast, there was no correlation between the degree of atherosclerosis and populations of circulating immature cells. Analysis of patients with cerebral artery occlusion revealed a significant positive correlation between circulating CD34- and CD133-positive cells and regional blood flow in areas of chronic hypoperfusion.

Conclusions—These results suggest a possible contribution of circulating CD34- and CD133-positive cells in maintenance of the cerebral circulation in settings of ischemic stress. Our data demonstrate the utility of a simple and precise method to quantify circulating CD34-positive cells, the latter providing a marker of cerebrovascular function. (***Circulation.* 2004;109:2972-2975.)

Key Words: cerebral infarction ■ cerebral ischemia ■ antigens, CD34 ■ stem cells

Although it had traditionally been assumed that replacement of damaged endothelium resulted only from outgrowth of preexisting vasculature, recent studies have identified endothelial progenitor cells (EPCs) that appear to contribute to vascular homeostasis and repair.[1] Clinical trials to assess the therapeutic potential of bone marrow–derived mononuclear cells, a rich source of immature cells including EPCs, in hind-limb[2,3] and cardiac ischemia[4] have been initiated and have, thus far, provided promising results. Furthermore, immature cells, including CD34-positive ($CD34^+$) cells, have been shown to contribute to maintenance of the vasculature, not only as a pool of EPCs but also as the source of growth/angiogenesis factors.[5] Bone marrow–derived immature cells have also been shown to participate in neovascularization of ischemic brain after experimental stroke.[6] On the basis of these results, we hypothesized that levels of circulating immature cells might be proportional to the resilience of the cerebral circulation to ischemic stress; ie, lower numbers of circulating immature cells might be associated with cerebral ischemia and infarction.

Methods

The institutional review board of the National Cardiovascular Center approved this study. All subjects provided informed consent. Circulating $CD34^+$ cells in 50 μL of peripheral blood were quantified according to the manufacturer's protocol (ProCOUNT, Becton Dickinson Biosciences). To minimize intersample variation for measurements of $CD34^+$ cells, several methods were used: A nucleic acid dye was added as a threshold reagent; a no-wash technique was performed to eliminate cell loss, and reverse pipetting was used; an internal reference particle was added for determination of absolute cell numbers; and an isotype control, matched for the concentration of anti-CD34 antibody and fluorochrome-to-protein ratio, was included. All measurements were performed in triplicate (Figure 1A, control; Figure 1B, CD34). To quantify other stem cell populations (besides $CD34^+$ cells), immature mononuclear cells were enriched

Received December 8, 2003; de novo received April 12, 2004; accepted May 11, 2004.

From the Departments of Cerebrovascular Disease (A.T., H.M., K.N., K.T., H.N.), Radiology and Nuclear Medicine (T.H., K.H.), and Clinical Physiology (K.M.), National Cardiovascular Center, Osaka, Japan; Department of Internal Medicine (T.M.), Hyogo College of Medicine, Hyogo, Japan; Dean's Office (D.M.S.), Medical College of Georgia, Augusta, Ga; and Department of Hematology (T.S.), Osaka Minami National Hospital, Osaka, Japan.

Correspondence to Akihiko Taguchi, Department of Cerebrovascular Disease, National Cardiovascular Center, 5-7-1 Fujishiro-dai, Suita, Osaka, 565-8565 Japan. E-mail ataguchi@res.ncvc.go.jp

Circulation is available at http://www.circulationaha.org

DOI: 10.1161/01.CIR.0000133311.25587.DE

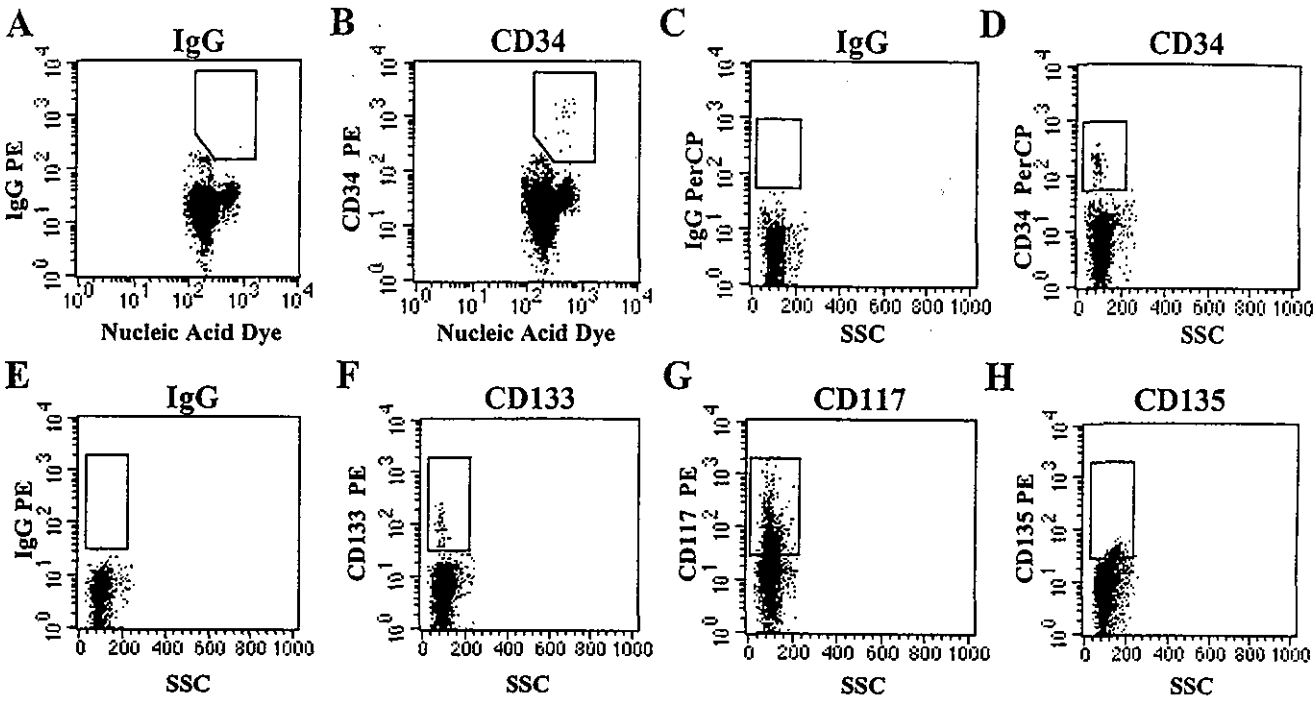

Figure 1. Quantification of circulating immature cells in patients with stroke. Nucleic acid dye versus CD34 PE dot plot was gated on lymphocytes and CD45 dim leukocytes. A, Results with an isotype-matched control antibody. B, Results with anti-CD34 antibody. Enriched immature mononuclear cells were double stained with PerCP-conjugated CD34 antibody (D) and PE-conjugated CD133 (F), CD117 (G), or CD135 (H) antibody. The number of cells in a region including brightly stained cells was counted. C and E, Staining with isotype nonimmune control antibody.

from 2 mL of peripheral blood by antibody-mediated depletion of mature cells according to the manufacturer's protocol (StemCell Technologies) using depletion cocktail, including antibodies to CD2, CD3, CD14, CD16, CD19, CD24, CD56, and CD66b. Enriched immature mononuclear cells were double-stained with peridinin chlorophyll protein (PerCP)-conjugated CD34 antibody (Figure 1D) and phycoerythrin (PE)-conjugated CD133 (Figure 1F), CD117 (Figure 1G), or CD135 (Figure 1H) antibody. The number of cells in a region including brightly stained cells was counted, and immature cells were quantified using $CD34^+$ cells as an internal control. The cumulative intra-assay coefficient of variation was 14%, 13%, 14%, and 15%, with $CD34^+$, $CD133^+$, $CD117^+$, and $CD135^+$ cell measurements, respectively, from 5 stroke patients.

Atherosclerosis in the common and internal carotid arteries was analyzed by ultrasonography to determine plaque score as described previously.[7] Cerebral infarcts (diameter >5 mm) were counted independently by a neurologist blinded to other parameters under study (number of circulating $CD34^+$, etc) using T1-weighted, T2-weighted, and fluid-attenuated inversion-recovery MRI obtained with a 1.5-Tesla MRI scanner. The diagnosis of hypoperfusion was made angiographically. Regional cerebral blood flow (CBF), cerebral blood volume, oxygen extraction fraction (OEF), and cerebral metabolic rate of oxygen ($CMRO_2$) were quantified by conventional steady-state ^{15}O PET using a PET scanner (Shimadzu) as described.[8] Cerebrovascular function was evaluated in patients with chronic hypoperfusion caused by major cerebral artery (carotid artery or M1 portion of the middle cerebral artery) occlusion or severe stenoses (>90%) without a major stroke. Twelve patients with 15 major arterial occlusions or stenoses had PET examinations.

To investigate the mobilization of immature cells after acute cerebral infarction, peripheral blood was quantified at 6 hours and 3, 7, 14, and 30 days after the onset of stroke. The episodes of acute cerebral infarction were confirmed by the diffusion image of brain MRI. Age-matched volunteers who had no history of cerebrovascular diseases and no neuronal deficiency were enrolled as controls (mean age, 67±4 years). Test-retest intraclass correlations were 0.88, 0.75, 0.86, and 0.86 for CD34, CD133, CD117, and CD135, respectively, obtained from 5 volunteers tested twice with an interval of at least 10 days between samples.

Univariant correlations were performed using Pearson's correlation coefficient and Spearman's correlation coefficient. Statistical comparisons among groups were determined using analysis of variance. Individual comparisons were performed using Students' *t* test. In all experiments, mean±SE is reported.

Results

First, we investigated mobilization of immature cells after acute cerebral infarction (n=5), focusing on $CD34^+$ cells. The level of $CD34^+$ cells gradually increased to day 7 and remained significantly above the prestroke baseline on days 7 and 14, returning to baseline levels by day 30 (Figure 2A). On the basis of these data, we enrolled 25 patients with a history of atherothrombotic cerebral ischemic events, excluding those who had suffered cerebrovascular or cardiovascular acute ischemic episodes in the 30 days before study, as well as premenopausal females. In this group (>30 days after stroke), no correlation was observed between the interval after stroke and the level of circulating $CD34^+$ cells (r=0.009, P=0.97). Characteristics of this group included mean age of 68±2 years, 20 men and 5 women, 23 patients receiving antiplatelet therapy, 11 patients receiving antihypertensive therapy, 6 patients receiving therapy for hyperlipidemia, 5 patients receiving therapy for diabetes mellitus (DM), and 16 patients with a current or past history of smoking.

Several factors were found to influence the number of circulating $CD34^+$ cells. Statistical analysis revealed a significant decrease in circulating $CD34^+$ cells in patients with DM (0.5±0.1; non-DM, 1.2±0.1 cells/μL; P=0.01). In contrast,

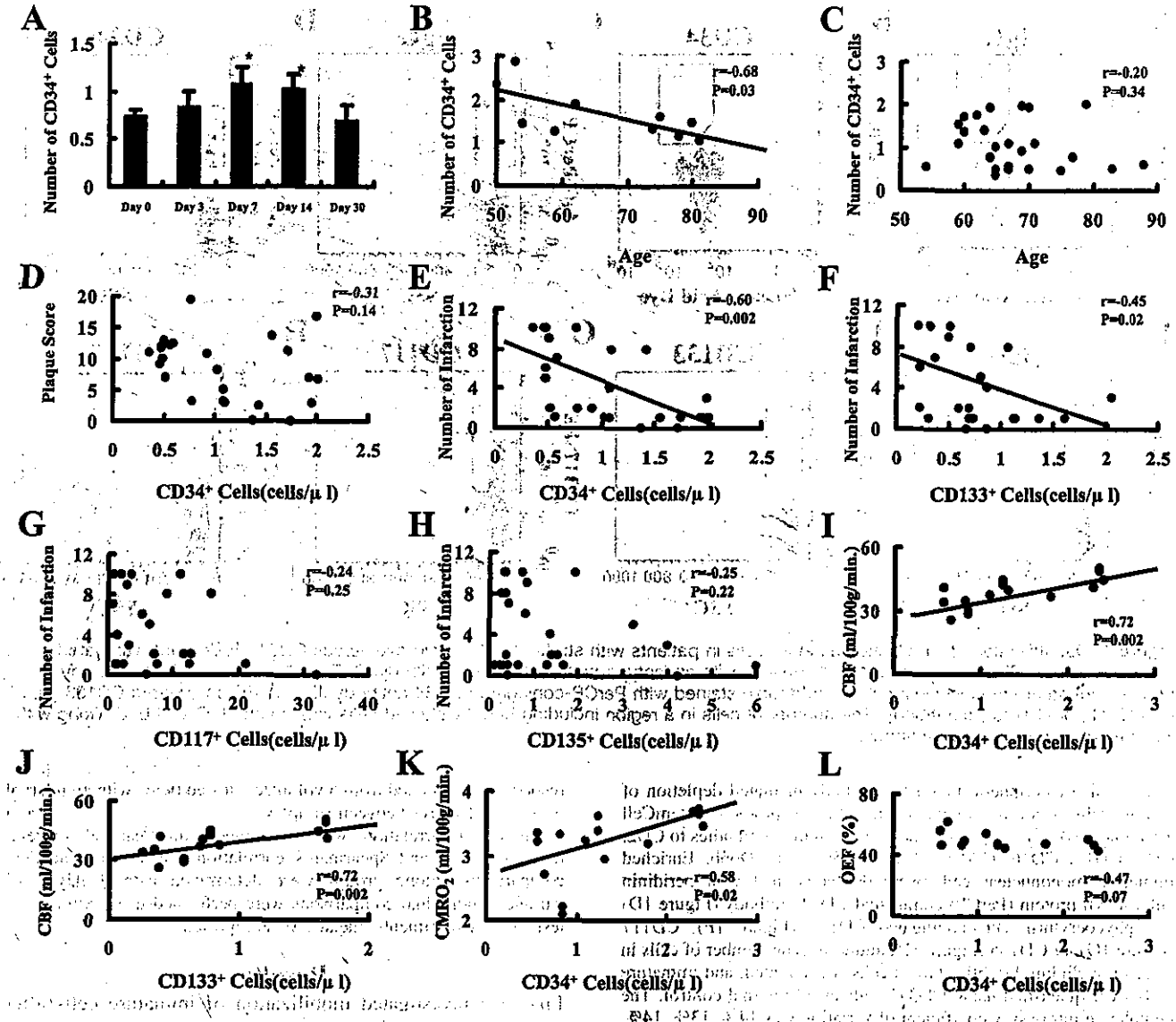

Figure 2. Levels of circulating CD34+ cells and stroke. Circulating CD34+ cells increased after the onset of stroke and peaked on day 7. A significant increase in circulating CD34+ cells was observed on days 7 and 14 (A). A decrease of circulating CD34+ cell was observed with aging in the control group (B), but no such correlation was observed in the stroke patient group (C). No correlation was observed between the number of circulating CD34+ cells and the degree of arteriosclerosis in major cerebral arteries (D). However, there was a correlation between cerebral infarctions and circulating CD34+ (E) and CD133+ cells (F). In contrast, there was no correlation between cerebral infarction and CD117+ (G) or CD135+ cells (H). Correlation between circulating CD34+ (I) and CD133+ (J) cells and CBF in areas of chronic hypoperfusion was observed. Lower levels of circulating CD34+ cells were correlated with a decrease in $CMRO_2$ (K) but not with a change in OEF (L). *$P<0.05$ compared with day 0 (based on 2-way ANOVA).

no change was observed in patients with hypertension ($P=0.61$), with hyperlipidemia ($P=0.81$), with smoking ($P=0.64$), or based on gender ($P=0.36$). In addition, treatment with HMG-CoA reductase inhibitors ($P=0.81$), compared with patients without hyperlipidemia, did not impact the number of CD34+ cells. In the control patient group, a decrease of circulating CD34+ cells was observed with aging (Figure 2B), although this was not observed in the patient group (Figure 2C). Comparing baseline levels of circulating CD34+ cells, there was a significant decrease in the patient group compared with age-matched controls (stroke, 1.1 ± 0.1; control, 1.6 ± 0.2 cells/μL; $P=0.02$).

We sought a possible correlation between circulating immature cells and the degree of arteriosclerosis of the common and internal carotid arteries in the patients with atherothrombotic cerebral ischemic events. However, there was no significant correlation between arteriosclerosis and circulating CD34+ (Figure 2D). This result was not surprising, because multiple risk factors and cell types contribute to progression of vascular lesions in major arteries. In contrast, because disruption of vascular homeostasis and repair are associated with cerebral infarction, we reasoned that a history of cerebral infarction might correlate with circulating immature cells. A strong correlation was observed between the number of infarcts and the absolute number of circulating CD34+ cells (Figure 2E) and CD133+ cells (Figure 2F). However, no significant correlation with regard to cerebral infarcts was observed with circulating CD117+ cells (Figure 2G) and CD135+ cells (Figure 2H).

In view of the critical role of endothelium in maintaining CBF, we evaluated cerebrovascular function in patients with chronic hypoperfusion. Direct correlations were observed between CBF (in the chronically hypoperfused area) and circulating CD34$^+$ cells (Figure 2I) and CD133$^+$ cells (Figure 2J). In addition, lower numbers of circulating CD34$^+$ cells (Figure 2K) correlated with diminished $CMRO_2$, although there was no significant increase in the OEF (Figure 2L). These observations suggest a contribution of CD34$^+$ cells in homeostasis and repair of the cerebral circulation and maintenance of brain metabolism. No correlation was observed with the above parameters of vascular function and circulating CD117$^+$ and CD135$^+$ cells. Measurement of angiogenic growth factors in patient plasma, vascular endothelial growth factor, basic fibroblast growth factor, hemopoietic growth factor, and insulin-like growth factor-1 also demonstrated no correlation with indices of cerebrovascular function or the number of CD34$^+$ cells (not shown).

Discussion

We have found that circulating immature cell populations, especially CD34$^+$ and CD133$^+$ cells, are associated with maintenance and repair of the cerebral vasculature. In our study, we used a simple and precise method to count the absolute number of circulating CD34$^+$ cells in a small sample of peripheral blood. Our results indicate that the level of CD34$^+$ cells serves as an index/marker for cerebrovascular function. Analysis of CD133$^+$, CD117$^+$, and CD135$^+$ cells, which identify other populations of immature cells, demonstrated that only CD133$^+$ cells correlated with cerebrovascular function in a manner paralleling CD34$^+$ cells.

Patients with diabetes displayed a significant reduction in the number of circulating CD34$^+$ cells. In view of the microvascular dysfunction that is characteristic of diabetes, this may not be surprising. Similarly, decreased circulating CD34$^+$ cells with increasing age in healthy individuals may be associated with limited vascular renewal in older individuals. It was also of interest to note no change between levels of CD34$^+$ cells in patients taking HMG-CoA reductase inhibitors. The latter results might reflect the positive effect of such drugs countering the negative effect of hyperlipidemia on circulating CD34$^+$ cells. Such conclusions, of course, are at best tentative, because in this first report we have identified associations rather than proved a cause-effect relationship.

These observations suggest that diminished numbers of CD34$^+$ and CD133$^+$ cells impact maintenance and repair of cerebral vasculature. Precise measurement of circulating CD34$^+$ cells provides a marker for cerebrovascular function in the setting of ischemic stress.

Acknowledgments

This work was supported by the Uehara, Takeda, Terumo Medical Foundations and KAKENHI (15590785). The sponsors of the study had no role in study design, data collection, data analysis, interpretation, or writing of the report.

References

1. Asahara T, Murohara T, Sullivan A, et al. Isolation of putative progenitor endothelial cells for angiogenesis. *Science*. 1997;275:964–967.
2. Taguchi A, Ohtani M, Soma T, et al. Therapeutic angiogenesis by autologous bone-marrow transplantation in a general hospital setting. *Eur J Vasc Endovasc Surg*. 2003;25:276–278.
3. Tateishi-Yuyama E, Matsubara H, Murohara T, et al. Therapeutic angiogenesis for patients with limb ischaemia by autologous transplantation of bone-marrow cells: a pilot study and a randomised controlled trial. *Lancet*. 2002;360:427–435.
4. Hamano K, Nishida M, Hirata K, et al. Local implantation of autologous bone marrow cells for therapeutic angiogenesis in patients with ischemic heart disease: clinical trial and preliminary results. *Jpn Circ J*. 2001;65: 845–847.
5. Majka M, Janowska-Wieczorek A, Ratajczak J, et al. Numerous growth factors, cytokines, and chemokines are secreted by human CD34$^+$ cells, myeloblasts, erythroblasts, and megakaryoblasts and regulate normal hematopoiesis in an autocrine/paracrine manner. *Blood*. 2001;97: 3075–3085.
6. Beck H, Voswinckel R, Wagner S, et al. Participation of bone marrow–derived cells in long-term repair processes after experimental stroke. *J Cereb Blood Flow Metab*. 2003;23:709–717.
7. Sasaki T, Watanabe M, Nagai Y, et al. Association of plasma homocysteine concentration with atherosclerotic carotid plaques and lacunar infarction. *Stroke*. 2002;33:1493–1496.
8. Hirano T, Minematsu K, Hasegawa Y, et al. Acetazolamide reactivity on ^{123}I-IMP single photon emission computed tomography in patients with major cerebral artery occlusive disease: correlation with positron emission tomography parameters. *J Cereb Blood Flow Metab*. 1994;14: 763–770.

International Congress Series 1270 (2004) 177–180

ELSEVIER

www.ics-elsevier.com

Prolonged interhemispheric neural conduction time evaluated by auditory-evoked magnetic signal and cognitive deterioration in elderly subjects with unstable gait and dizzy sensation

Hiroshi Oe[a,*], Akihiko Kandori[b], Tsuyoshi Miyashita[b], Kuniomi Ogata[b], Naoaki Yamada[c], Keiji Tsukada[d], Kotaro Miyashita[a], Saburo Sakoda[e], Hiroaki Naritomi[a]

[a] *Department of Cerebrovascular Medicine, National Cardiovascular Center, 5-7-1 Fujishiro-dai, Suita, Osaka 565-8565, Japan*
[b] *Central Research Laboratory, Hitachi Ltd., Tokyo, Japan*
[c] *Department of Radiology, National Cardiovascular Center, Osaka, Japan*
[d] *Okayama University, Okayama, Japan*
[e] *Department of Neurology, Osaka University, Osaka, Japan*

Abstract. Magnetoencephalography (MEG) studies have showed that the latency of auditory-evoked neuronal action peak (N100m peak) detected at the temporal cortex ipsilateral to the auditory stimulation is delayed as compared with that detected at the contralateral side. Our recent auditory evoked magnetic fields (AEFs) study has indicated that auditory impulses, originated from the unilateral ear, first arrive at the contralateral temporal cortex and later reach the ipsilateral temporal cortex through interhemispheric neural connections, thus leading to the delay of ipsilateral N100m peak latency. Such a conduction pathway of auditory impulses makes it possible to measure interhemispheric neural conduction time (INCT). We measured INCT in 33 elderly patients (72 ± 10 years of age) complaining of unstable gait and dizzy sensation to study its relationship with cognitive function. Cognitive function was estimated with mini-mental state examination (MMSE) scores. The patients were classified into two groups, such as Group A with normal cognitive function (MMSE score ⩾ 24, $n = 23$) and Group B with cognitive dysfunction (MMSE score ⩽ 23, $n = 10$). INCT was significantly longer in Group B (50.5 ± 14.7 ms) than in Group (15.6 ± 13.9 ms, $p < 0.05$). In the entire patient group, INCT was prolonged negatively correlating with MMSE scores ($r = -0.84$, $p < 0.001$). The results of the present study suggest that the impairment of cognitive function may be closely related with the prolongation of

* Corresponding author. Tel.: +81-6-6833-5012; fax: +81-6-6872-7486.
E-mail address: hirooe@hsp.ncvc.go.jp (H. Oe).

doi:10.1016/j.ics.2004.05.090

INCT. The measurement of INCT with AEFs may be useful for early detection of cognitive impairment in elderly patients with dizziness who may later develop dementia.

Keywords: Auditory evoked magnetic fields; N100m peak latency; Cognitive deterioration; Mini-mental state examination; Dizziness

1. Introduction

Auditory impulses, originating from the unilateral ear, reach the temporal auditory cortex bilaterally [1], although detailed neural pathways are unknown. MEG studies have indicated that the latency of auditory-evoked neuronal action peak (N100m peak) detected at the temporal cortex ipsilateral to the auditory stimulation is always delayed as compared with that detected at the contralateral side [2]. Regarding this phenomenon, our recent MEG study has suggested that auditory impulses originating from the unilateral ear first arrive at the contralateral temporal cortex and later reach the ipsilateral temporal cortex through interhemispheric neural connections, thus leading to the delay of ipsilateral N100m peak latency [3]. Such a conduction manner of auditory impulses enables us to measure interhemispheric neural conduction time (INCT) with MEG. We estimated the INCT, using MEG, in elderly patients with unstable gait and dizziness and studied its relationship with cognitive function.

2. Subjects and methods

2.1. Subjects

Thirty-three patients (18 males and 15 females, 72 ± 10 years of age) complaining of unstable gait and dizzy sensation, who had otherwise no focal neurological abnormality, were subjected. We excluded patients with auditory impairments at 30 dB or less in 1000 Hz pure tone audiograms or abnormal findings in otorhinologic examinations, caloric test and auditory brain stem response.

2.2. Methods

MEG studies were performed using a superconducting quantum interference device (SQUID) system (MC-6400, Hitachi) with 64 co-axial gradiometer (8×8 matrix) in a two-dimensional plane. Auditory stimuli with 90 dB normal hearing level in intensity and 1 kHz tone burst were provided in the right ear, and N100m peak latency was measured at both temporal cortices (Fig. 1). Cognitive function was estimated by measurement of the mini-mental state examination (MMSE) score. The patients were classified into two groups, according to MMSE scores as follows: Group A with normal cognitive function (MMSE scores $\geqslant 24$) and Group B with cognitive dysfunction (MMSE scores $\leqslant 23$). The INCT (ms) was calculated from the

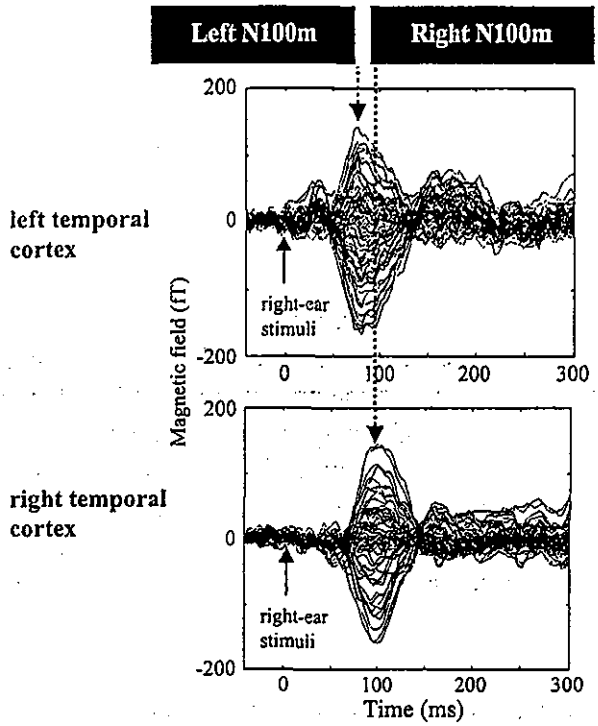

Fig. 1. Left N100m and right N100m peak latencies in a patient (right-ear stimuli). Interhemispheric neural conduction time (INCT) (ms) = right N100m peak latency – left N100m peak latency.

right and left N100m peak latencies. The INCT was compared between the two groups.

3. Results

MMSE scores were normal in 23 patients (Group A: MMSE score 24–30; 71 ± 12 years of age) and reduced in 10 patients (Group B: MMSE score 19–23; 73 ± 6 years of age). The ages in the two groups were the same. With the right ear stimuli, the N100m peak latency at the left temporal cortex was almost the same in Group A (92.8 ± 15.3 ms) and Group B (93.9 ± 13.9 ms), whereas the N100m peak latency at the right temporal

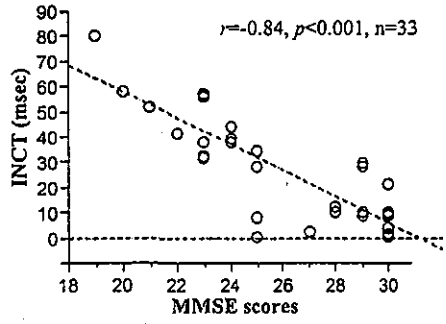

Fig. 2. The relationship between MMSE scores and interhemispheric neural conduction time (INCT) in 33 patients (right ear stimuli).

cortex was significantly longer in Group B (143.3 ± 13.7 ms) than in Group A (109.3 ± 16.7 ms, $p<0.01$). The INCT was significantly longer in Group B (50.5 ± 14.7 ms) than in Group A (15.6 ± 13.9 ms, $p<0.05$). When analyzed in the entire patient group, there was a significantly negative correlation between MMSE scores and INCT ($r=-0.84$, $p<0.001$) (Fig. 2).

4. Discussion

Cognitive function takes place under rapid interactions of multiple cerebral regions interconnected with neurons. The results of the present study suggest that cognitive function may deteriorate correlating with the prolongation of INCT in elderly patients with unstable gait and dizziness. The INCT may represent the time required for the inter-regional neural process to perform cognitive function. Dizziness is related with gait unstableness that is known to be a predictor of non-Alzheimer's dementia. The measurement of INCT with AEFs may be useful for early detection of cognitive impairment in elderly patients with unstable gait and dizziness who may later develop dementia.

Acknowledgements

This study was supported by a Grant-in-Aid for Scientific Research No. 13072601, supported by the Ministry of Health, Welfare and Labor of Japan.

References

[1] C.M. Hackney, Anatomical features of the auditory pathway from cochlea to cortex, Br. Med. Bull. 43 (1987) 780–801.
[2] C. Pantev, et al., Study of the human auditory cortices using a whole-head magnetometer: left vs. right hemisphere and ipsilateral vs. contralateral sitmulation, Audiol. Neuro-otol. 3 (1998) 183–190.
[3] H. Oe, et al., Interhemispheric connection of auditory nerural pathways assessed by auditory evoked magnetic fields in patients with fronto-temporal lobe infarction, Neurosci. Res. 44 (2002) 483–488.

Available online at www.sciencedirect.com
SCIENCE DIRECT
Neuroscience Research 49 (2004) 253–260
Neuroscience Research
www.elsevier.com/locate/neures

Quantitative magnetic detection of finger movements in patients with Parkinson's disease

Akihiko Kandori [a,*], Masaru Yokoe [b], Saburo Sakoda [b], Kazuo Abe [b], Tsuyoshi Miyashita [c], Hiroshi Oe [d], Hiroaki Naritomi [d], Kuniomi Ogata [c], Keiji Tsukada [e]

[a] *Central Research Laboratory, Hitachi Ltd., Life Science Research Laboratory, 1-280 Higashi-Koigakubo, Kokubunji-shi, Tokyo 185-8601, Japan*
[b] *Department of Neurology, Osaka University Medical School, Osaka, Japan*
[c] *Advanced Research Laboratory, Hitachi Ltd., Bio and Medical Solution Laboratory, Osaka, Japan*
[d] *Department of Cerebrovascular Medicine, National Cardiovascular Center, Osaka, Japan*
[e] *Department of Electrical and Electronic Engineering, Okayama University, Okayama, Japan*

Received 22 January 2004; accepted 5 March 2004

Abstract

To develop a new measurement tool for quantitatively detecting the finger movement of a patient with Parkinson's disease (PD), we designed a magnetic sensing system consisting of a magnetic induction coil, a sensing coil, and a circuit unit. The sensing coil detects the inducted magnetic field that varies with the distance between the two coils, and the detected signals are demodulated in the circuit unit in order to obtain the variation voltage from the oscillation frequency. To obtain a coefficient for converting voltage to distance, we measured the output voltages for seven fixed finger positions of 12 normal volunteers. The voltage differences corresponding to the finger movement in 20 PD patients, six age-matched controls, and 12 normal volunteers were then recorded for 30 s. To investigate the velocity and acceleration of the finger movement, we calculated their waveforms from the measured displacement waveform. We also detected the main frequency of the tapping rhythm by using a fast Fourier transform (FFT). The averaged amplitude of each waveform decreased with the disorder in the Hoehn–Yahr (HY) stage, while the averaged tapping frequency of PD patients did not have any correlation with this stage. It can be concluded that this magnetic sensing system can assess finger movement quantitatively.

Keywords: Parkinson's disease; Finger tapping; Magnetic detection

1. Introduction

The most prominent clinical feature of Parkinson' disease is movement disability including rigidity, tremor, bradykinesia, akinesia, and disturbances of rhythm formation. Since the assessment of these symptoms depends on the skill of individual neurologists, a common objective assessment is needed.

It has been suggested that the basal ganglia facilitate sequential movement, engaging subsequent movements in a movement sequence (Marsden, 1990), and the bradykinesia and disturbances of rhythm formation that occur in Parkinson's disease (PD) are usually assessed by using a finger-tapping test. The finger movement in finger-tapping tests has been analyzed by electrical-switch tapping (Shimoyama et al., 1990), metal-loop tapping (Freeman et al., 1993), keyboard tapping (Giovannoni et al., 1999; Homann et al., 2000; Bronte-Stewart et al., 2000), and three-dimensional optoelectronic camera tracking (Konczak et al., 1997; Agostino et al., 2003). The methods other than the one using an optoelectronic camera system, however, can analyze only the bradykinesia and incoordination of the index finger because they can monitor only the movement of 'on' and 'off'. Furthermore, the data processing of the optoelectronic camera system is very complex because of the use of a two-dimensional image. There has been no study on sequential-motion analysis of finger-to-thumb opposition using a simple apparatus.

We therefore developed a new apparatus for quantitatively studying the dynamics of finger movement by using data

* Corresponding author. Tel.: +81-42-323-1111x3922; fax: +81-42-327-7783.
E-mail address: kandori@crl.hitachi.co.jp (A. Kandori).

0168-0102/$ – see front matter
doi:10.1016/j.neures.2004.03.004

obtained from a magnetic sensor. This apparatus is small enough for use in a consultation room or by the bedside. The main purpose of the work reported here was to determine whether this apparatus could be used to objectively assess the symptoms of patients with Parkinson' disease. A major advantage of our magnetic sensor is that it enables the degree of finger opening and the incoordination of finger-to-thumb oppositions to be analyzed without being affected by involuntary movement including tremors. This sensor can also sensitively detect the subtle finger movement of hastened taps.

2. Materials and methods

2.1. Subjects

The subjects in this study were 12 healthy volunteers (six male and six female) between 26 and 43 years old, 20 Parkinson's patients (10 male and 10 female) between 46 and 82 years old, and six age-matched controls (three male and three female) between 62 and 89 years old. We classified the PD patients into five stages based on the Hoehn–Yahr (HY) stage system (Hoehn and Yahr, 1967). HY-I patients had effects on one side of the body, HY-II patients had effects on both sides of the body, HY-III patients showed impairments in balance and walking, HY-IV showed marked impairments in balance and walking, and HY-V patients were completely immobile. Informed consent was obtained from all subjects. The 12 volunteers also participated in calibration experiments determining the relation between movement distance and output voltage of the new measurement tool (see Section 2.3).

2.2. Configuration of magnetic detection system

The magnetic detection system (Fig. 1) consists of oscillation and detection coils (each 14 mm in diameter and comprising 30 loops of copper wire), a circuit unit (170 mm × 120 mm × 50 mm), and a personal computer. The oscillator and one amplifier in the circuit unit produce a 100-mA ac current (20 kHz) that flows through the oscillation coil, producing a magnetic field oscillating at the same frequency. The magnetic field inducts a voltage with the same frequency in the detection coil. This voltage is amplified by a pre-amplifier and fed to a phase-shift detector to be demodulated by using a 20-kHz reference signal whose phase was adjusted because the inducted signal has a phase delay. The output of the phase-shift detector is run through a low-pass filter (corner frequency = 30 Hz) and amplified. The final output is digitized at 100 Hz by an analog-digital (AD) board in the computer.

The oscillation and detection coils are attached to the thumb and index finger with two-sided tape as shown in Fig. 1b and connected by a twisted lead wire 1 m long to the circuit unit, whose output is recorded by the notebook personal computer with the AD board. The data size for a 30-s recording is only 7 kB.

2.3. Measurement of the relationship between output voltage and movement distance

The thumb and index finger are not always parallel during finger-tapping, and the strength of detected magnetic field is not linearly related to the distance over which the fingers move because its magnitude is inversely proportional to the square of the distance between the oscillation and detection coils. Calibration data are therefore needed to determine the movement distance.

Using the six male and six female healthy volunteers, we measured the output signals for movement distances of 0, 20, 40, 60, 80, 100, and 120 mm. After investigating the difference between male and female subjects and the difference between left and right fingers in the calibration data (see Section 3), we used this data to convert the output signals obtained with all subjects to movement distances.

2.4. Finger-tapping measurement

We measured the output signals due to the finger movement of each hand of all subjects (12 healthy volunteers, six age-matched controls, and 20 PD patients) for 30 s. These subjects were instructed to tap as rapidly as possible while moving their fingers as far as they could. All subjects practiced tapping before the measurement so they could make the finger movements correctly.

2.5. Data analysis

The measured tapping waveforms included almost no artifacts due to movements such as tremor of the fingers. We therefore think that finger precise velocity and acceleration can be estimated accurately from the measured waveforms.

Thirty seconds of data digitized at 100 Hz were stored in the PC. The stored voltage was converted to movement distance D by using the calibration data given in Section 2.4, and the velocity and acceleration of the finger movements were calculated from the derivatives of (dD/dt and d^2D/dt^2). The waveforms for movement distance, velocity, and acceleration were used to determine the differences between the finger movements of healthy volunteers and PD patients. The differences were evaluated by calculating a displacement value (i.e., |maximum value| − |minimum value|) in each waveform during the 30-s period.

We analyzed the tapping rhythm by using the fast Fourier transform (FFT). Before the FFT algorithm was used, the mean value of the 30-s data (3000 points) was subtracted from a raw waveform in order to determine the tapping frequency. And the main cyclic timing was determined by finding the frequency with the highest peak in the obtained power spectrum.

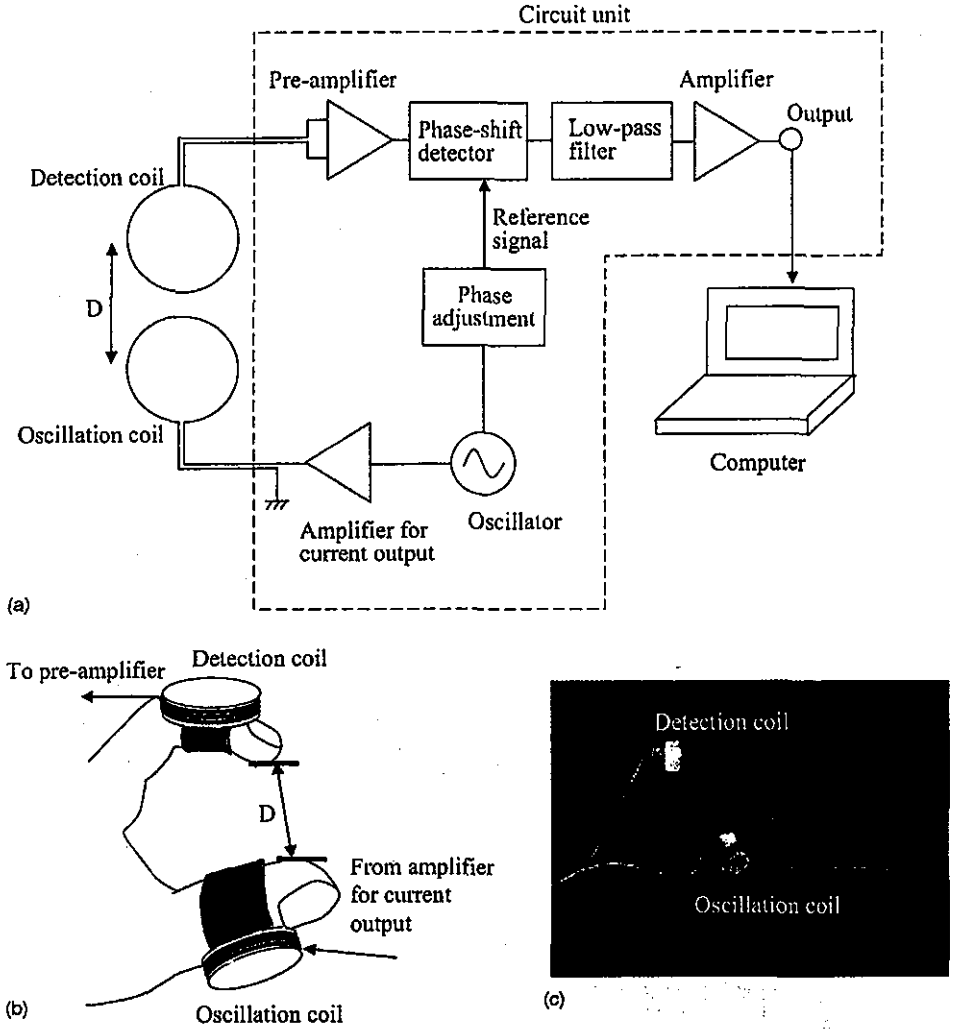

Fig. 1. (a) Block diagram of the magnetic detection system; (b) configuration of detection and oscillation coils. D is the movement distance between the index finger and thumb; and (c) photograph of detection and oscillation coils attached to the fingers by two-sided tape.

3. Results

The output voltages measured to obtain the calibration data are summarized in Table 1, where the difference between male and female subjects is seen to be not significant for either hand. Furthermore, the values for the right and left hand are also very similar at each distance. The calibration data was therefore simplified by averaging all 12 volunteers' data for each position. The averaged data are plotted in Fig. 2, which shows that the output voltage decreases with increasing distance D. The voltage waveform was changed to the movement-distance waveform by using the interpolated line shown in Fig. 2.

Table 1
Output voltages measured for seven movement distances D in 12 young volunteers

Right hand				Left hand		
D (mm)	Male ($n = 6$)	Female ($n = 6$)	P-value	Male ($n = 6$)	Female ($n = 6$)	P-value
0	−2.2 ± 0.2	−3.0 ± 0.4	NS	−2.2 ± 0.3	−2.8 ± 0.4	NS
20	−1.1 ± 0.2	−1.3 ± 0.1	NS	−1.1 ± 0.2	−1.4 ± 0.3	NS
40	−0.55 ± 0.2	−0.54 ± 0.1	NS	−0.51 ± 0.09	−0.57 ± 0.08	NS
60	−0.28 ± 0.08	−0.27 ± 0.06	NS	−0.27 ± 0.05	−0.29 ± 0.02	NS
80	−0.16 ± 0.04	−0.16 ± 0.04	NS	−0.16 ± 0.02	−0.15 ± 0.02	NS
100	−0.098 ± 0.02	−0.094 ± 0.02	NS	−0.093 ± 0.008	−0.090 ± 0.01	NS
120	−0.062 ± 0.01	−0.056 ± 0.01	NS	−0.057 ± 0.004	−0.061 ± 0.01	NS

The difference between female and male is not significant for any distance, and the left- and right-hand data are very similar. P-value: Pearson t-test.

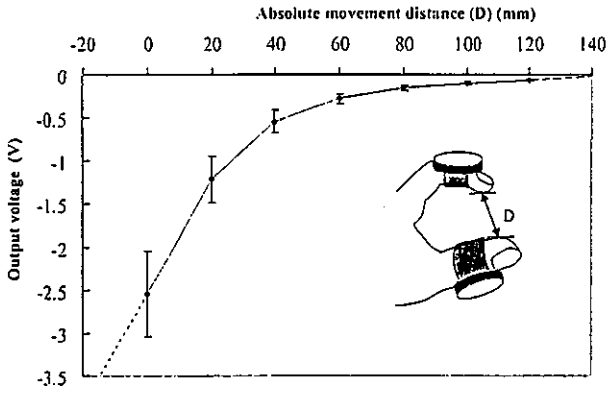

Fig. 2. Relation between movement distance D and the output voltage of the magnetic detection system. The relation is plotted by averaging all 12 volunteers data (including both left- and right-hand data). The averaged relation is in inverse proportion.

To compare the calibrated waveform with the raw waveform, see the two waveforms for a normal case that are drawn in Fig. 3. The voltage waveform near a 0 V does not include detailed movement, but the calibrated waveform (Fig. 3b) gives more detailed information.

Distance, velocity, and acceleration waveforms for a healthy volunteer are shown in Fig. 4. Although the amplitude of the distance waveform is constant, the amplitudes of the velocity and acceleration waveforms decrease. This pattern was evident in the waveforms for all the healthy volunteers. The distance, velocity, and acceleration amplitudes (|maximum value| − |minimum value|) and main tapping frequencies (determined as shown in Fig. 5) for the healthy volunteers are listed in Table 2. All parameters (D, dD/dt, d^2D/dt^2, and F) have no significant value in males and females, although female's d^2D/t^2 is slight smaller than those of males.

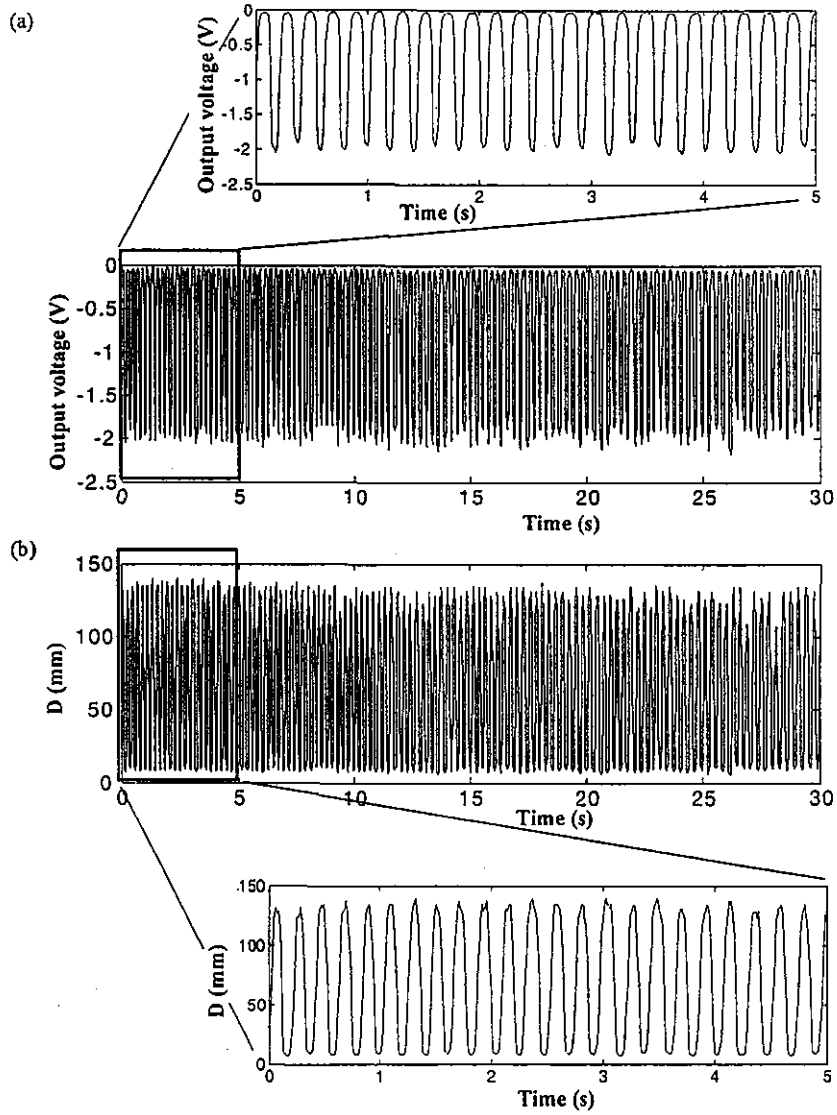

Fig. 3. (a) Output voltage waveform of magnetic detection system in the case of a young healthy volunteer. The wave near 0 V does not reflect a detailed motion and (b) movement-distance waveform changed from (a). The wave reflects a real finger motion.

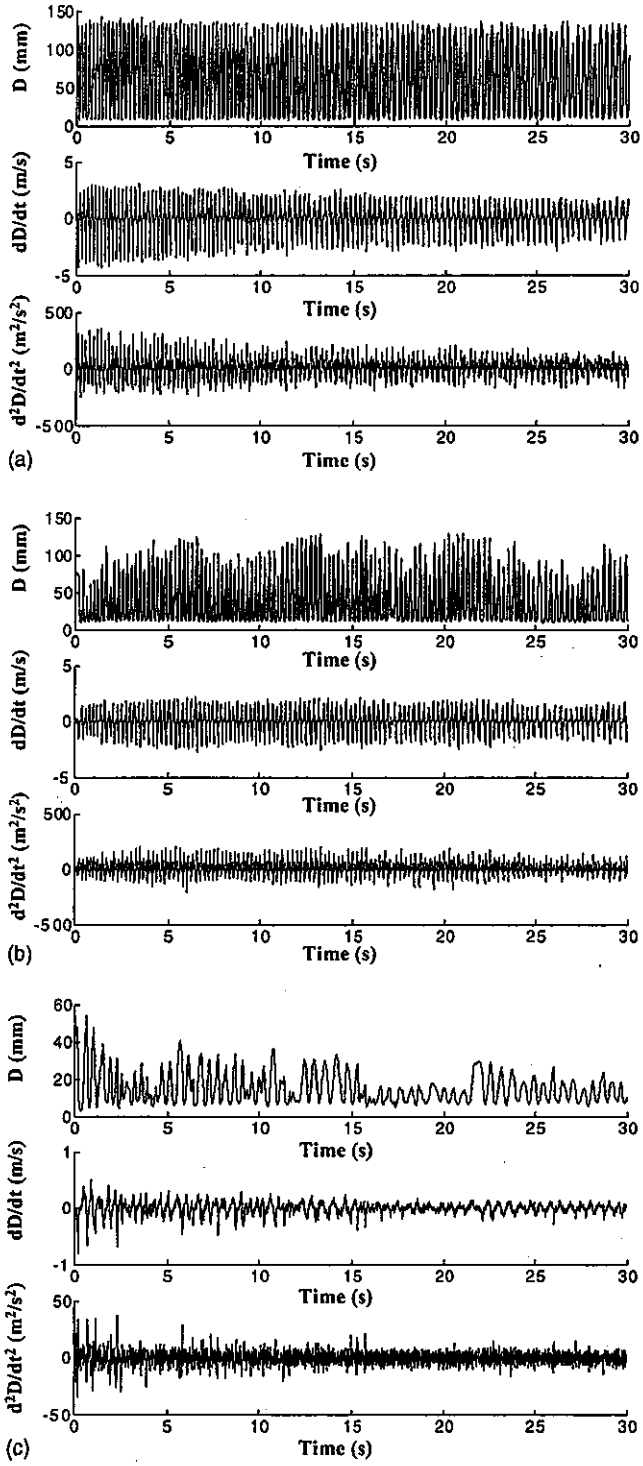

Fig. 4. (a) Movement-distance waveform of a young healthy volunteer. (The waveform is the same as that in Fig. 3b.) Velocity waveform calculated from the distance waveform. Acceleration waveform calculated from the waveform the velocity waveform; (b) movement-distance waveform of age-matched elderly control. Velocity waveform calculated from the distance waveform. Acceleration waveform calculated from the velocity waveform; (c) movement-distance waveform of PD patient (HY-III). Velocity waveform calculated from the distance waveform. Acceleration waveform calculated from the velocity waveform.

The amplitudes of the velocity and acceleration waveforms for the age-matched normal control were roughly constant (as shown in Fig. 4b), but the amplitude of the distance waveform for the age-matched normal control varied more than that of the younger normal volunteers did.

Typical distance, velocity, and acceleration waveforms of a Parkinson-disease patient are shown in Fig. 4c. The amplitude of each varies arrhythmically.

Power spectra calculated from the movement-distance waveforms of a control and a PD patient are shown in Fig. 5. The highest peak in each is the main frequency F; it is 4.3 Hz for the control and 1.8 Hz for the PD patient. The power spectrum for the PD patient is also shown on an expanded scale, since its magnitude is much less than that of the power spectrum for the control.

For all subjects in this study, the average displacement value (|maximum value| − |minimum value|) in each waveform (D, dD/dt, and d^2D/dt^2) during the 30 s is plotted in Fig. 6 along with the average main frequency F. All values are shown with their standard deviations. The amplitudes of the average displacements plotted in Fig. 6a–c decrease as the HY stage becomes more severe. Furthermore, the amplitude of each displacement value differs significantly between the young and old volunteers. The averaged main frequency, on the other hand, is weakly correlated with the HY stage. Furthermore, the deviation of the main frequency is very large.

4. Discussion

In this study, we have demonstrated the possibility of quantitatively detecting finger-movement disorders in PD patients by using a magnetic sensor system. This apparatus can easily measure the degree of finger opening and the incoordination of finger-to-thumb oppositions. In this report, we cannot show the effect of involuntary movements (e.g., tremors) because none of our subjects was afflicted with tremors. Note, however, that the sensor would hardly detect tremors because the finger-to-thumb distance does not vary greatly during tremor. Therefore, we can directly observe finger opening and incoordination of finger-to-thumb oppositions.

Using the magnetic detection system, we found that the mean values of three parameters (D, dD/dt, and d^2D/dt^2) decrease as the severity of Parkinson symptoms (as indicated by the patient's HY stage) increases. The main frequency, on the other hand, is more weakly correlated with the severity of a patient's symptoms. The decrease in these three parameters reflects an increasing degree of dyskinesia, such as muscle stiffness and loss of strength. A kinesia score decrease in accordance with the HY stage has been reported by investigators using the total number of computer keystrokes (Homann et al., 2000). The keystroke number is identified from the main frequency in Fig. 6d. Their results (with a large distribution in kinesia score)

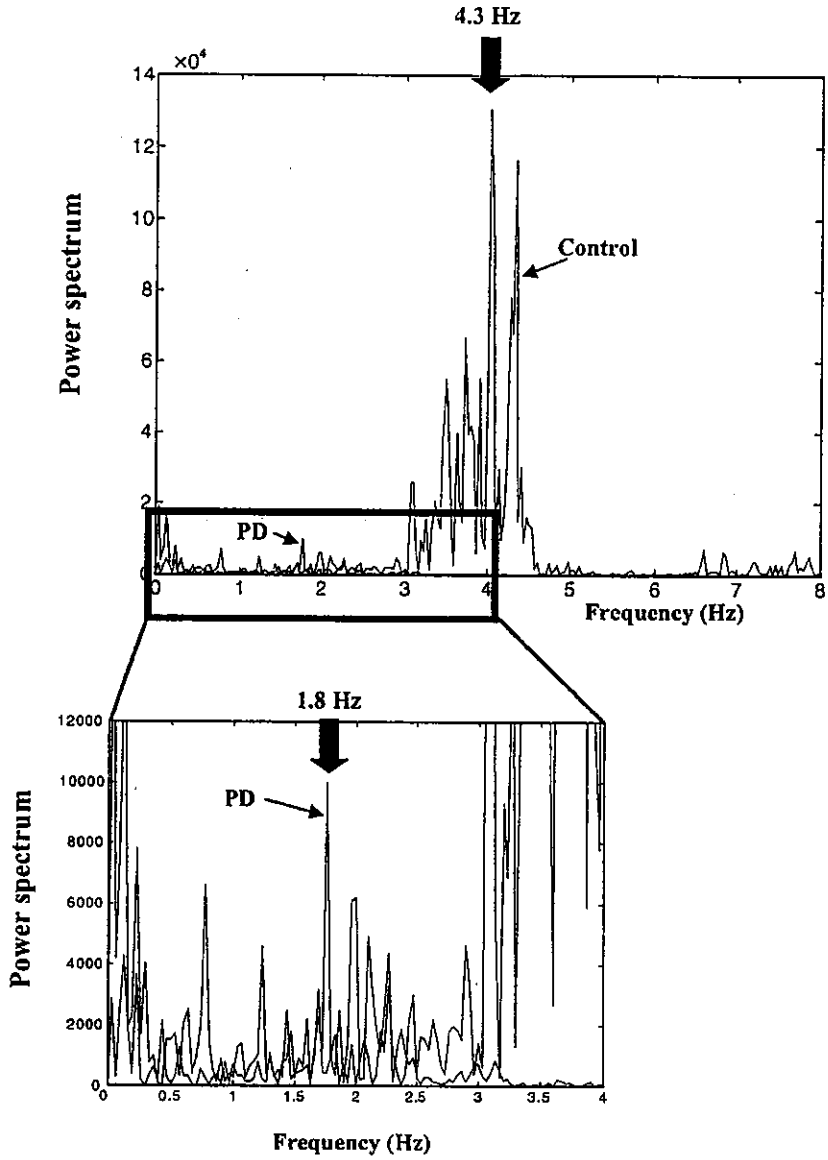

Fig. 5. Power spectra calculated from the movement-distance waveforms of a typical control (red line) and a HY-III PD patient (blue line). The main frequency is 4.3 Hz in the control's power spectrum and 1.8 Hz in the PD patient's power spectrum. Furthermore, the magnitude of the PD's spectrum is much weaker than that of the control's power spectrum.

are very similar to our findings. It can thus be considered that the magnetic-sensor system can determine a kinesia score.

Furthermore, it must be noted that the parameters D, dD/dt, and d^2D/dt^2 for our young volunteers (averaging 32.5 years old) are much larger than those of our elderly controls (averaging 71.3 years old). This significant difference is caused by a deterioration of the brain motor function with age. The deterioration has been reported by investigators using tapping frequency (Shimoyama et al., 1990). In their results and ours (Fig. 6d), the tapping frequencies of young people cannot be distinguished from those of elderly people. The parameters D, dD/dt, and d^2D/dt^2 of young people, however, can be distinguished from those of elderly people. This clear discrimination might indicate that our magnetic detection system can accurately detect the deterioration of motor function.

None of the output voltages obtained from the 12 healthy volunteers differed between sexes or the right and left hands at any of the movement distances (Table 1). This shows the size of the hand and the fingers has little effect on this magnetic detection system. We need, however, to consider the maximum possible distance between the thumb and the index finger because a size-dependence of this distance might affect the parameters used to evaluate the degree of motor disorder in Parkinson patients.

In summary, the simple magnetic detection system we developed for the finger-tapping test can be used to assess the severity of PD patient symptoms quantitatively.

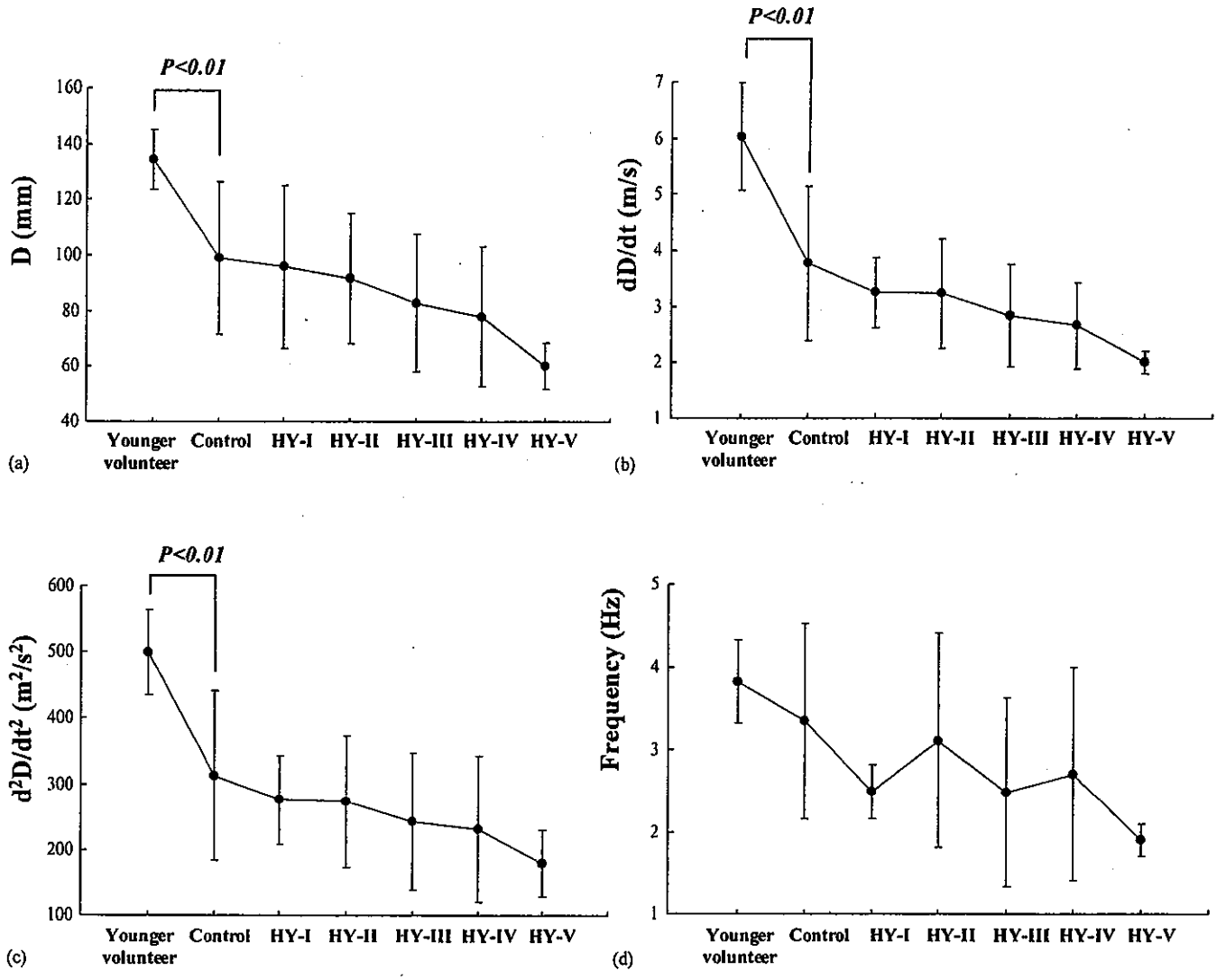

Fig. 6. (a) Maximum displacement of the movement-distance D. (b) Maximum replacement of the velocity (dD/dt). (c) Maximum displacement of the acceleration (d^2D/dt^2). (d) Main frequency F. In (a), (b), and (c), the mean values decrease with the degree of disorder. In (d), the main frequency has a similar tendency.

Furthermore, it may also offer a new strategy for treatment of these patients.

4.1. Limitations of this study

There are several limitations of this study. First, a comparison with many age-matched patients and controls is needed. Second, to obtain more detailed information, a new identification parameter for detecting disorders such as an arrhythmic repetitive movement may be needed. Third, the effect of the maximum possible distance between thumb and the index finger should be taken into account when the simple magnetic-detection method we developed is used. Despite these limitations,

Table 2
List of three parameters (D, dD/dt, and d^2D/dt^2) in 12 young volunteers

	Left hand			Right hand		
	Male ($n = 6$)	Female ($n = 6$)	P-value	Male ($n = 6$)	Female ($n = 6$)	P-value
D (mm)	137 ± 4	134 ± 18	NS	133 ± 6	134 ± 15	NS
dD/dt (m/s)	6.6 ± 0.8	5.5 ± 1.2	NS	6.5 ± 0.8	5.5 ± 1.0	NS
d^2D/dt^2 (m^2/s^2)	554 ± 53	460 ± 75	NS	546 ± 58	437 ± 72	NS
F (Hz)	3.7 ± 0.3	3.8 ± 0.5	NS	4.0 ± 0.7	3.8 ± 0.5	NS

The difference between female and male is not significant for any parameter. Furthermore, left- and right-hand data are very similar.

however, the method is very useful for measuring finger movement.

Acknowledgements

We gratefully thank Minoru Sakairi, Kenkou Uchida, and Hideo Kawaguchi of Hitachi Ltd. for their helpful comments.

References

Agostino, R., Currà, A., Giovannelli, M., Modugno, N., Manfredi, M., Berardelli, A., 2003. Impairment of individual finger movements in Parkinson's disease. Mov. Disord. 18 (5), 560–592.

Bronte-Stewart, H.M., Ding, L., Alexander, C., Zhou, Y., Moore, G.P., 2000. Qunatitative digitography (ODG): a sensitive measure of digital mortor control in idiopathic Parkinson's disease. Mov. Disord. 15 (1), 36–47.

Freeman, J.S., Cody, F.W.J., Schandy, W., 1993. The influence of external timing cues upon the rhythm of voluntary movements in Parkinson's disease. J. Neural Neurosurg. Psychiatry 56, 1078–1084.

Giovannoni, G., van Schalkwyk, J., Fritz, V.U., Lees, A.J., 1999. Bradykinesia akinesia inco-ordination test (BRAIN TEST): an objective computerized assessment of upper limb motor function. J. Neural Neurosurg. Psychiatry 67, 624–629.

Hoehn, M.M., Yahr, M.D., 1967. Parkinsonism: onset. Neurology 17, 427–442.

Homann, C.N., Suppan, K., Wenzel, K., Giovannoni, G., Ivanic, G., Horner, S., Ott, E., Hartung, H.P., 2000. The bradykinesia akinesia incoordination test (BRAIN TEST), an objective and user-friendly means to evaluate patients with Parkinsonism. Mov. Disord. 15 (4), 641–647.

Konczak, J., Ackermann, H., Hertrich, I., Spieker, S., Dichgans, J., 1997. Control of repetitive lip and finger movment in Parkinson's disease: influence of external timing signals and simultaneous execution on motor performance. Mov. Disord. 12 (5), 665–676.

Marsden, C.D., 1990. Neurophysiology. In: Stern, G.M. (Ed.), Parkinson's disease. Chapman and Hall Medical, London, pp. 57–98.

Shimoyama, I., Ninchoji, T., Uemura, K., 1990. The finger tapping: quantitative analysis. Arch. Neurol. 47, 681–684.

Predictors of Clinical Outcome in Patients Receiving Local Intra-Arterial Thrombolysis without Subsequent Symptomatic Intracranial Hemorrhage against Acute Middle Cerebral Artery Occlusion

Tatsuro Takada, Masahiro Yasaka, Kazuo Minematsu,
Hiroaki Naritomi, and Takenori Yamaguchi

BACKGROUND AND PURPOSE: **The factors that predict favorable outcome after local intra-arterial thrombolysis (LIT) remain unknown. We aimed to clarify these factors in patients with middle cerebral artery occlusion treated by LIT.**

METHODS: **We performed LIT in 26 consecutive patients who had middle cerebral artery occlusion with a modified Rankin scale (mRS) score ≤2 before stroke onset. We assessed background characteristics, angiographic findings, and mRS score at discharge. We compared these factors between patients with good outcome (mRS score, ≤2) and those with poor outcome (mRS score, ≥3).**

RESULTS: **The duration from symptom onset to hospital admission was 0.96 ± 0.87 (mean ± SD) hour and from onset of stroke to LIT was 3.78 ± 1.17 hours. No patients developed symptomatic intracerebral hemorrhage or died. Thirteen patients achieved good outcomes. No significant differences existed between the two groups in baseline National Institutes of Health Stroke Scale (NIHSS) scores, time from stroke onset to LIT, blood pressure, early CT signs, or subsequent hemorrhagic transformation shown by CT. However, univariate analysis showed that patients with good outcomes were younger, more often had absence of hypertension history, had better collaterals shown by angiography, and had better recanalization rates than those with poor outcomes. NIHSS scores after LIT were lower in patients with good outcomes than in patients with poor outcomes. Logistic regression analysis indicated improvement of the NIHSS scores by ≥2 immediately after LIT was independently associated with good outcome.**

CONCLUSION: **Improvement of the NIHSS score by ≥2 immediately after LIT is a useful predictor of patient outcome at discharge.**

In 1995, the National Institute of Neurologic Disorders and Stroke rt-PA Stroke Study Group reported that IV thrombolytic therapy using recombinant tissue plasminogen activator (rt-PA) within 3 hours of ischemic stroke onset improved patient outcomes (1). However, a randomized trial that used rt-PA within 6 hours of onset failed to show the therapeutic efficacy (2). No benefits were shown in the Alteplase Thrombolysis for Acute Noninterventional Therapy in Ischemic Stroke study (known as the ATLANTIS Trial), a randomized controlled trial with patients receiving rt-PA from 3 to 5 hours after onset (3). Therefore, the American Heart Association guidelines for acute ischemic stroke recommend that the IV administration of rt-PA has to begin within 3 hours of onset (4). On the other hand, local intra-arterial thrombolysis (LIT) was reported to be efficacious in patients with middle cerebral artery (MCA) occlusion if performed within 6 hours of onset. In the Prolyse in Acute Cerebral Thromboembolism II study, LIT improved the prognosis of stroke within 6 hours of onset (5).

In 6% to 20% of patients who undergo thrombolysis, a serious side effect of symptomatic intracerebral hemorrhage (SICH) develops (1–6). SICH in patients

Received January 13, 2004; accepted after revision March 7.
This study was supported in part by Research Grants (15C-1 for Cardiovascular Disease, H14-shinkin-007) from the Ministry of Health, Labor and Welfare of Japan.
From the Cerebrovascular Division, Department of Medicine, National Cardiovascular Center, Osaka, Japan.
Address reprint requests to Tatsuro Takada, MD, Cerebrovascular Division, Department of Medicine, National Cardiovascular Center, 5-7-1 Fujishirodai, Suita, Osaka 565-8565, Japan.

receiving rt-PA was found to be related to tissue plasminogen activator dose, National Institute of Health Stroke Scale (NIHSS) score, and diastolic blood pressure (7, 8).

Early ischemic changes revealed by CT, such as cortical effacement (9), were also involved in the occurrence of SICH. The American Heart Association guidelines warn about the administration of rt-PA in patients with high blood pressure and early signs revealed by CT (4). We performed LIT in patients with acute MCA occlusion during the past 4 years in a prospective study design. We strictly adhered to predefined inclusion and exclusion criteria, and no patient developed SICH. Our purpose was to determine which clinical factors are predictors of favorable outcome.

Methods

Inclusion and Exclusion Criteria

The clinical inclusion criteria for LIT were acute embolic stroke within 6 hours of symptom onset, patient age from 20 to 85 years, and NIHSS score from 5 to 29. The exclusion criteria included the following: 1) neurologic symptoms caused by subarachnoid hemorrhage, neoplasm, septic embolism, moyamoya disease, or vasculitis; 2) seizure at onset; 3) rapidly improving neurologic signs at any point before LIT; 4) history of stroke within the previous 4 weeks (except transient ischemic attacks); 5) surgery, biopsy, or trauma with internal injuries within 2 weeks; 6) active or recent hemorrhage within 2 weeks; 7) baseline international normalized ratio of prothrombin time >1.7 or baseline platelet count $<10 \times 10^4$/L; 8) uncontrolled hypertension defined by systolic blood pressure >185 mmHg or diastolic blood pressure >100 mmHg; 9) pregnancy or puerperal period. CT of the brain exclusion criteria included intracranial tumor, hemorrhage, and an early sign revealed by CT (acute hypoattenuated parenchymal lesion) in more than one-third of the MCA territory.

In patients who satisfied all the clinical and CT inclusion criteria, diagnostic cerebral angiography was performed. The angiographic exclusion criteria were occlusion of the internal carotid artery or long segment basilar artery occlusion and aneurysms or arterial dissections.

From April 1997 to December 2001, we screened 364 patients by using cerebral angiography. We found internal carotid artery occlusion in 51 patients, MCA occlusion in 135, basilar artery occlusion in 13, cerebral artery dissections in eight, cerebral aneurysms in eight, and other arterial occlusion or no occlusion in the other 149. Forty-seven patients (mean age, 66.4 ± 11.6 years; men, 35; women, 12) who were diagnosed as having MCA occlusion based on cerebral angiography findings within 6 hours of symptom onset were admitted to our Stroke Care Unit. Excluded were 18 patients: one with a malignant tumor, one with rapid improvement of symptoms before cerebral angiography, three who were older than 85 years, two with high blood pressure, and 11 with early CT signs involving more than one-third of the MCA territory. The remaining 29 patients underwent LIT. None of the 29 patients developed SICH or died during the hospital stay. Three of the 29 patients were not independent (modified Rankin scale score, ≥3) before the index stroke. We analyzed the remaining 26 patients who had modified Rankin scale (mRS) scores <2 before stroke onset.

Thrombolytic Procedure and Post-LIT Treatment

We performed cerebral angiography via a femoral approach. The LIT was performed when clinical, CT, and angiographic criteria were completely met and written informed consent was obtained from the patient or a family member. An infusion microcatheter with a single end hole was placed on the distal portion of the MCA thrombus by using a steerable microguidewire through a 6-French guiding catheter. Maximum dose of 420,000IU of urokinase (Urokinase 60,000IU, Mitsubishi Pharma Corporation) was infused manually at the rate of 35 mL/hr through the microcatheter. Simultaneously, mechanical disruption of the clot was performed by using a flexible microguidewire with a tip angle of 90 degrees (GT wire TERMO, 0.016 or 0.012 in). Penetration and fragmentation of the thrombus were achieved by gently advancing and rotating the tip of microguidewire. The LIT was stopped when the infusion time from the start of LIT exceeded 1 hour or when the operator confirmed that the artery was recanalized by >50% of the area perfused by the initial occluded artery during capillary, as seen in the lateral view.

The protocol required that no anticoagulants or antiplatelet agents were administered for 24 hours after treatment and that arterial blood pressure was monitored during the first 24 hours. When systolic blood pressure increased to >180 mmHg after LIT, IV antihypertensive drugs were continuously infused for at least 48 hours.

Clinical Variables and Outcome Measures

We assessed a history of hypertension (previous systolic ≥160 mmHg or diastolic ≥95 mmHg or receiving antihypertensive drugs), diabetes mellitus (fasting blood sugar >7.7 mmol/L, random blood sugar >11.1 mmol/L, or receiving insulin or oral hypoglycemic agents), hypercholesterolemia (total cholesterol ≥220 mg/dL or receiving antihyperlipidemic agents), smoking or alcohol habit, and anticoagulant and antiplatelet therapy before stroke onset. Grades of collateral flows and vessel recanalization were assessed by using cerebral angiography. All the angiograms were analyzed by a stroke neurologist without knowing the final result. The grades of collaterals were simply classified as poor (<50% of the occluded vascular territory was caused by collaterals) and good (collateral flows via leptomeningeal anastomoses allowed >50% filling of the territory distal to the occlusion). The achieved vessel recanalization was classified as described by Mori et al (10) and Yamaguchi et al (11). Vessel recanalization was classified into two groups. The lesion was categorized to be low grade if no or slight recanalization was perfusing <50% of the ischemic area. The grade of vessel recanalization was considered to be high grade when reperfusion covering >50% of the ischemic area was achieved.

Early signs revealed by initial CT were defined on the basis of loss of insular ribbon and cortical ribbon effacement. The presence or absence of hemorrhagic transformation was evaluated by follow-up CT performed >24 hours after LIT. SICH was diagnosed when hemorrhagic transformation was confirmed by CT and NIHSS score increased by ≥4 or when level of consciousness deteriorated by 1 point compared with before LIT.

Neurologic severity was assessed immediately, at 24 hours, and at 1 month after LIT by using NIHSS scores. Outcome at discharge was assessed by using the mRS and the Barthel index scores. Number of deaths during the hospital stay was monitored.

Statistical Analysis

All values are expressed as mean ± SD for parametric values or as a median (range) for nonparametric values. Comparisons among groups were made by analysis of variance and then Mann-Whitney U test. The χ^2 test was conducted for the analysis of discrete variables. $P < 0.05$ was considered to be statistically significant. Logistic regression analysis was used to evaluate the contribution of the various factors to the outcome.